Salvador Rubio, FJ.; Martínez López, JE.; Romero Bauset, JV.; Roselló Ferragud, MD. (2014). Study of the influence of the needle eccentricity on the internal flow in diesel injector nozzles by computational fluid dynamics calculations. International Journal of Computer Mathematics. 91(1):24-31. doi:10.1080/00207160.2013.770483.

International Journal of Computer Mathematics
Vol. 00, No. 00, January 2008, 1–9

RESEARCH ARTICLE. Special Issue: Jornadas 2012b

Study of the influence of the needle eccentricity on the internal flow in diesel injector nozzles by CFD calculations

F.J. Salvador[†,*], J. Martínez-López[†], J.-V. Romero[‡] and M.-D. Roselló[‡]

[†]*CMT-Motores Térmicos, Universitat Politècnica de València, Camino de Vera s/n, Edificio 6D, 46022 Valencia, Spain,*
Tel. Num. 0034-963877650, Fax Num. 0034-963877659;
[‡]*Instituto de Matemática Multidisciplinar, Universitat Politècnica de València, Camino de Vera s/n, Edificio 8G, 2°, 46022 Valencia, Spain,*
Tel. Num. 0034-963877007, Ext. 88289

(*October 2012*)

In the present paper, a computational study has been performed in order to clarify the effects of the needle eccentricity in a real multihole microsac nozzle. This nozzle has been simulated at typical operating conditions of a diesel engine, paying special attention to the internal flow development and cavitation appearance within the discharge orifices. For that purpose, a multiphase flow solver based on a homogeneous equilibrium model with a barotropic equation of state has been used, introducing the turbulence effects by RANS methods with a RNG k-ε model. The results obtained from this investigation have demonstrated the huge influence of the needle position on the flow characteristics, showing important hole to hole differences.

Keywords: diesel injector, cavitation, needle eccentricity, internal flow

AMS Subject Classification: 76M12; 76T99

1. Introduction

It is well known that during the opening and closing process of a diesel injector, the fuel characteristics at the nozzle exit change significantly as a consequence of the needle movement [8, 14, 15]. This change of fluid properties at the exit of the discharge orifices due to the variable position of the needle strongly affects the spray pattern and the air-fuel mixing process, and therefore its subsequent combustion [5, 6, 10, 12, 13].

Nevertheless, despite most investigations focus only on the vertical motion of the needle, the internal flow and spray characteristics can be also affected by an eccentric location of the needle [4, 9]. This phenomenon, produced by random oscillations of the needle in the transverse direction during the opening or closing of the injector, makes difficult the study of the internal flow, especially at cavitating conditions. Indeed, the existence of a multiphase flow, together with the small dimensions of the nozzles and the high velocities reached within their discharge orifices make the use of CFD tools the best alternative to advance in this area.

*Corresponding author. Email: fsalvado@mot.upv.es

ISSN: 0020-7160 print/ISSN 1029-0265 online

DOI: 0020716YYxxxxxxxx
http://www.informaworld.com

Cavitation modeling can be dealt with three different approaches: interface tracking models [16], two fluid models [2] and single-phase models [7, 11]. Interface tracking methods treat the liquid and vapour phases separately solving one set of governing equations for each phase and solving the interface independently. Two fluid models treat also the liquid and vapour phases separately, solving one set of governing equations for each phase but modeling the interaction between them with an additional source term. Single-phase models, also called continuum flow models, consider the fuel at liquid and vapour phases as a homogeneous mixture, solving only one set of equations. This kind of models, together with a barotropic equation of state seems to be the most suitable method to model the internal flow in diesel injector nozzles [7, 11].

The present work has been structured in the following way. Firstly, a brief description of the code used and its main equations will be given. Secondly, the nozzle and the operating conditions simulated will be presented in section 3. Then, the cavitation appearance and the flow properties of each orifice will be analyzed in detail. Moreover, in this section the total fuel injected and the averaged momentum flux and effective velocity will be also studied. Finally, the main conclusions of the study will be drawn in section 5. The nomenclature used throughout the paper is given in the appendix.

2. Cavitation Modelling

The code used in the present work for modelling the internal flow at cavitating conditions was rasCavitatingFoam, implemented in OpenFOAM [1]. This model belongs to continuum nozzle flow models or homogeneous equilibrium models (HEMs), which assume that liquid and vapour are always perfectly mixed in each cell. Precisely, for calculating the amount of vapour in each cell it uses the parameter X, defined as:

$$X = \frac{\rho - \rho_{\mathrm{l\,sat}}}{\rho_{\mathrm{v\,sat}} - \rho_{\mathrm{l\,sat}}}. \tag{1}$$

The main equations of the code are the continuity equation (Eq. (2)), the momentum equation (Eq. (3)) and a common barotropic equation of state (Eq. (4)), which relates pressure and density,

$$\frac{\partial \rho}{\partial t} + \nabla \cdot (\rho \boldsymbol{u}) = 0, \tag{2}$$

$$\frac{\partial (\rho \boldsymbol{u})}{\partial t} + \nabla \cdot \left(\rho \frac{\boldsymbol{u}\boldsymbol{u}}{2}\right) = -\nabla p + \nabla \cdot (\mu \nabla \boldsymbol{u}) - \nabla \tau, \tag{3}$$

$$\frac{\mathrm{D}\rho}{\mathrm{Dt}} = \Psi \frac{\mathrm{Dp}}{\mathrm{Dt}}. \tag{4}$$

For relating density and pressure, the model uses the compressibility of the mixture, which is the inverse of the speed of sound square:

$$\Psi = \frac{1}{a^2}. \tag{5}$$

This value, as happen for the calculation of the fuel viscosity, is determined with a linear model in accordance to the amount of vapour in each cell and the fluid properties at liquid and vapour phases:

$$\Psi = X \cdot \Psi_{\mathrm{v}} + (1 - X) \cdot \Psi_{\mathrm{l}}, \tag{6}$$

$$\mu = X \cdot \mu_{\mathrm{v}} + (1 - X) \cdot \mu_{\mathrm{l}}. \tag{7}$$

On the other hand, the high velocities achieved in diesel injection nozzles (up 600 m/s) force to take into account the turbulence effects. For that reason a RNG k-ε model has been used, which introduces two new transport equations: one for the turbulent kinetic energy and a second one for the energy dissipation,

$$\frac{\partial(\rho k)}{\partial t} + \frac{\partial(\rho k u_i)}{\partial x_i} = \frac{\partial}{\partial x_j}\left[\left(\mu + \frac{\mu_{\mathrm{T}}}{\sigma_k}\right)\frac{\partial k}{\partial x_j}\right] + P_k - \rho\varepsilon, \tag{8}$$

$$\frac{\partial(\rho\varepsilon)}{\partial t} + \frac{\partial(\rho\varepsilon u_i)}{\partial x_i} = \frac{\partial}{\partial x_j}\left[\left(\mu + \frac{\mu_{\mathrm{T}}}{\sigma_\varepsilon}\right)\frac{\partial \varepsilon}{\partial x_j}\right] + C_{1\varepsilon}\frac{\varepsilon}{k}P_k - C_{2\varepsilon}\rho\frac{\varepsilon^2}{k}, \tag{9}$$

where $C_{1\varepsilon} = 1.42$, $C_{2\varepsilon} = 1.68$ and $\sigma_k = \sigma_\varepsilon = 0.72$.

3. Nozzle description and operating conditions

In order to study the influence of the needle eccentricity on the internal flow, two different geometries have been simulated: one nozzle with a needle perfectly centered and a second one with an eccentric position of the needle (displaced 70 µm). Both geometries belong to the same diesel injector nozzle, which has 6 cylindrical holes with a length of 1 mm, a diameter of 170 µm and a curvature inlet radius of 13 µm. These internal characteristics were obtained by an experimental technique based on special moulds of silicone [11].

The geometries created from the silicone technique results are depicted in Figure 1. In both cases the nozzle have been modeled at fully needle lift conditions (250 µm) [3] and they have been discretized in a hybrid mesh of around 600000 hexahedral cells. The cell size ranges from 7.5 µm in the orifice core to a minimum of 2 µm in the orifice wall. For the rest of the geometry (sac, needle seat, etc.) the cell size range from 7.5 µm to 22.5 µm depending on the distance between the needle and the nozzle wall.

As far as the boundary conditions are concerned, five pressure conditions have been tested. The injection pressure, defined as the pressure existing in the common rail, was set with a constant value of 30 MPa. This value belongs to low injection pressures for current diesel engines, but ensure different cavitation intensities using typical pressures of the combustion chamber (backpressures). The backpressures simulated to achieve it were 1, 3, 5, 7 and 9 MPa. Unlike the injection pressure, the backpressure has not been adjusted with a constant value, but with a mean value. This kind of boundary condition allows the existence of pure vapour in the nozzle outlet, since it allows areas with a pressure lower than the predefined backpressure keeping the mean value desired in all the section.

With regard to the fuel simulated, the properties set in the model belong to a diesel fuel Repsol CEC RF-06-99 at 23°C. Its properties, obtained experimentally,

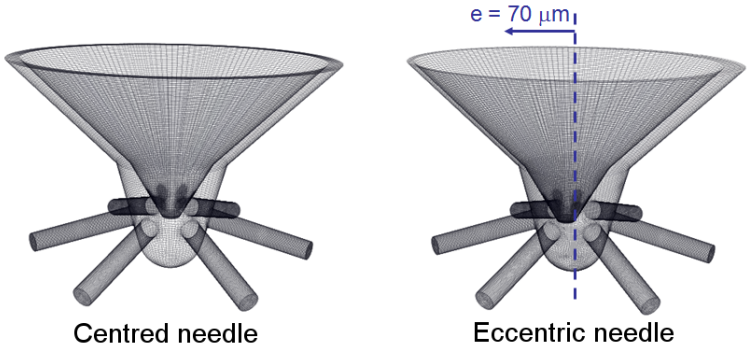

Figure 1. Geometries simulated: nozzle with a needle perfectly centred (left) and with an eccentric position (right).

are a density at liquid phase of 830 kg/m^3 and a viscosity value of 0.0033 kg/ms. However, due to the difficulties to obtain the properties for the vapour phase, they were adjusted using the values given by Karrholm et al. [7].

4. Influence on the internal flow

In order to make easier the analysis of the results obtained from the simulations, they have been organized in three different sections. The first one deals with the cavitation appearance of each orifice for both geometries. The second sections focus on the hole to hole deviations in terms of mass flow and momentum flux and their causes. Finally, the flow properties at the nozzle exit, considering the total mass flow injected by the nozzle and the averaged values of all the orifices for the velocity and momentum flux are analyzed in the third item.

4.1 *Cavitation appearance*

Analyzing the cavitation appearance, there are not hole to hole differences for the nozzle with the needle placed in the center. As a sample, Figure 2 shows how cavitation starts in the curvature radius of the orifice inlet and grows mainly along the upper part of the hole until reaching the nozzle exit. This cavitation field is exactly the same for the rest of orifices.

For the case with an eccentric position of the needle, the fact of having a variable pressure field in the nozzle depending on the needle position affects the cavitation development. Indeed, if the isosurfaces for $X \geq 0.1$ are analyzed for each orifice, it is clear that the vapour phase distribution is completely different. For holes 4 and 5 the entry of fuel from the upstream area and from the sac, forces that cavitation reaches the outlet from the upper and lower part of the hole. However, as the entry of fuel in the orifices 1 and 2 from the sac is lower, the cavitation developed in the lower part of the orifice is almost negligible.

Once understood the cavitation development for orifices 1–2 and 4–5, it is quite easy to understand the vapour phase developed in the orifices 3 and 6. The amount of fuel coming in these orifices by their bottom part is lower than the orifices 4–5 and higher than the orifices 1–2. For that reason, the cavitation length in the lower part of the orifice is between the length observed in the orifices 1–2 and 4–5. Another important aspect to remark is the fact that the vapour film does not follow the direction of the orifice axis. This last phenomenon is a consequence of the different pressure and velocity distribution upstream the orifice (see Figure 3).

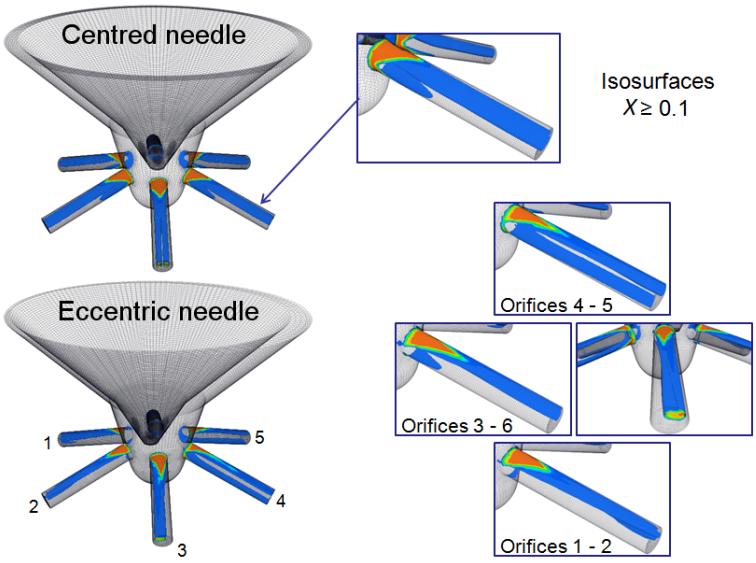

Figure 2. Cavitation fields at P_{inj} = 30 MPa − P_{back} = 1 MPa.

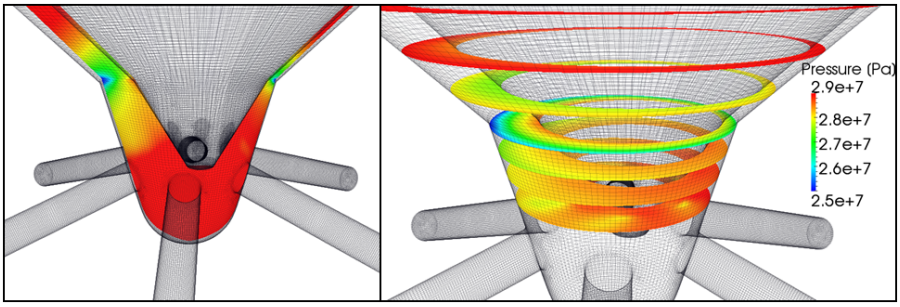

Figure 3. Pressure fields for the case with the eccentric needle. P_{inj} = 30 MPa − P_{back} = 1 MPa.

4.2 *Hole to hole deviation*

Obviously, for the case where the needle is placed in the center of the nozzle the values of mass flow, momentum flux and effective velocity are the same for all the orifices. Nevertheless, as can be seen in Figure 4 corresponding to the eccentric needle case at P_{back} = 1 MPa, the mass flow and momentum flux values strongly depend on the needle position.

On the upper right part of Figure 4 there is a nozzle scheme with all the orifices labeled for making easier the explanation of the results, being the orifices number 1 and 2 the orifices closer to the needle and the orifices 4 and 5 the farthest ones. Surprisingly, the mass flow and momentum flux in the orifices closer to the needle (the orifices 1 and 2) are higher, being the orifices 4 and 5, which are the farthest from the needle, the holes with less momentum and mass flow. This behavior can be explained as a consequence of the cavitation field seen and explained in Figure 2, since the existence of vapor in the upper and lower part of the orifices 4 and 5 strongly reduces the amount of fuel injected.

4.3 *Total/averaged flow properties*

Figure 5 shows the total mass flow (considering all the orifices of the nozzle) and the averaged momentum flux and effective velocity at the nozzle outlet as a function

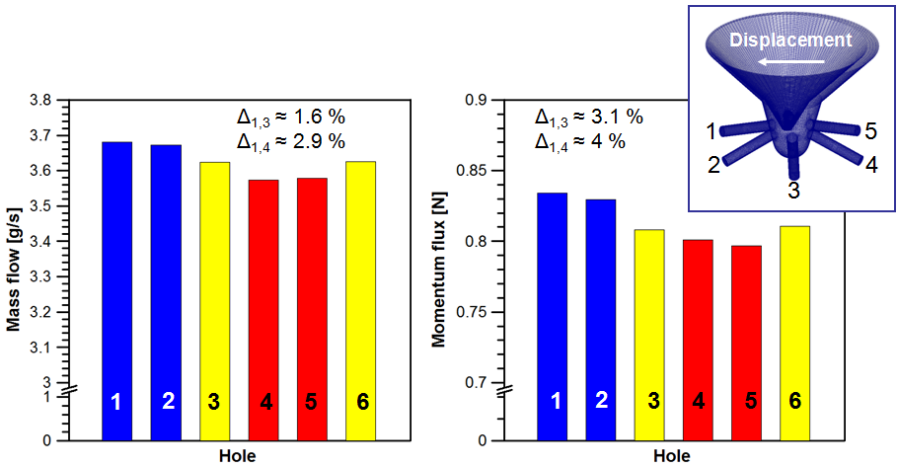

Figure 4. Pressure fields for the case with the eccentric needle. P_{inj} = 30 MPa − P_{back} = 1 MPa.

of the square root of pressure drop. Pressure drop (ΔP) is defined as the difference between the injection pressure and the backpressure. The higher the backpressure, the lower the pressure drop. As the injection pressure is kept to 30 MPa, backpressures of 1, 3, 5, 7 and 9 MPa, lead to square root of pressure drop values of 5.4, 5.2, 5, 4.8 and 4.6 $MPa^{0.5}$ respectively. The number beside the different points represented in the three plots of Figure 5 represents the value of backpressure.

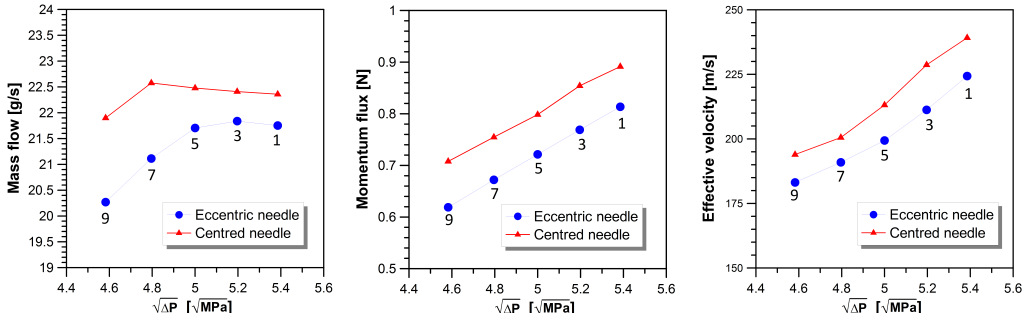

Figure 5. Mass flow, momentum flux and effective velocity results.

Attending to the mass flow graph, the amount of fuel injected in the combustion chamber for the case where the needle is perfectly placed increases as the backpressure decreases from 9 to 5 MPa. Once the backpressure arrives to 5 MPa, the mass flow remains chocked or collapsed, and despite decreasing the discharge pressure the mass flow remains invariable. This phenomenon is a consequence of phase change of the fuel from liquid to vapour due to cavitation [11].

For the nozzle with an eccentric position of the needle, the critical cavitation conditions or the conditions where the mass flow starts to be constant is achieved at a higher backpressure (7 MPa). However, not only the evolution of the flow is different between both cases, but also the values obtained. Indeed for all the pressure conditions the amount of fuel injected is higher when the needle is placed in the center of the nozzle, with a maximum difference of around 7.4 % for the highest backpressures (9 MPa).

With regard to the averaged momentum flux at the nozzle outlet, the trend of this parameter is similar in both cases with a continuous increase of the force of the spray with the pressure drop. As happened with the mass flow results, the comparison of momentum flux values between both cases shows important

differences, being the averaged momentum flux of the orifices when the needle is centered 12 % higher.

This tendency can be seen also analyzing the effective velocity of the flow in the outlet section of the orifices, since for all the pressure conditions the velocity when the needle is displaced is 7 % lower.

Effective velocity is obtained by dividing the momentum flux by the mass flow as established by Payri et al. [12].

From this graph it is also interesting to notice the increase of the slope when cavitation takes place (at 7 MPa and lower backpressures for the centered needle case and 5 MPa and lower backpressures for the eccentric needle case). This behavior has two explanations: on the one hand, as there are vapour bubbles in the flow, the cross section for the pass of fluid is lower; on the other hand, as the viscosity of the vapour phase is lower, the friction losses decreases [11].

5. Summary and conclusions

The effects of the needle eccentricity in a diesel injection nozzle have been studied with a multiphase flow solver based on a homogeneous equilibrium model with a barotropic equation of state. For that reason two different geometries have been simulated at real operating conditions of diesel engines: one nozzle with its needle perfectly centered and another one with an eccentric displacement of its needle of 70 µm.

From this analysis, the following conclusions can be drawn:

- When the needle is perfectly centered, the cavitation appearance is similar in all the orifices, whereas if the needle is displaced there are strong variations of the vapour phase between orifices.
- The eccentricity of the needle produces strong hole to hole differences in terms of mass flow, momentum flux and effective velocity.
- In overall terms, an eccentric position of the needle produces lower values of mass flow, momentum flux and effective velocity.

Acknowledgements

This work was partly sponsored by “Vicerrectorado de Investigación, Desarrollo e Innovación” of the “Universitat Politècnica de València” in the frame of the project “Estudio de la influencia del uso de combustibles alternativos sobre el proceso de inyección mediante GRID computing (FUELGRID)”, and by “Ministerio de Ciencia e Innovación” in the frame of the project “Estudio teórico-experimental sobre la influencia del tipo de combustible en los procesos de atomización y evaporación del chorro Diesel (PROFUEL), reference TRA2011–26293. This support is gratefully acknowledged by the authors.

The authors would also like to thank the computer resources and assistance provided by the Universidad de Valencia in the use of the supercomputer “Tirant”.

Nomenclature

a: speed of sound
$C_{1\varepsilon}$: constant for ε transport equation calculation
$C_{2\varepsilon}$: constant for ε transport equation calculation

D: diameter
k: turbulent kinetic energy
p: pressure
P_{back}: back pressure
P_{inj}: injection pressure
P_{k}: production of turbulent kinetic energy
t: time
$\boldsymbol{u}$: velocity
X: vapour fraction

Greek symbols:

ε: turbulence dissipation rate
ΔP: pressure drop, ΔP=$P_{\text{inj}} - P_{\text{back}}$
μ: fluid viscosity
μ_{T}: turbulent viscosity
σ_ε: constant for ε transport equation calculation
σ_k: constant for k transport equation calculation
ρ: fluid density
$\rho_{\text{l sat}}$: liquid density at saturation
$\rho_{\text{v sat}}$: vapour density at saturation
τ: Sub-Grid Scale-Stress
Ψ: fluid compressibility

Subscripts:

l: liquid
v: vapour

References

[1] OpenCFD® is a registered trade mark, http://www.opencfd.co.uk/.
[2] A. Alajbegovic, G. Meister, D. Greif, and B. Basara, *Three phase cavitating flows in high-pressure swirl injectors*, Experimental Thermal and Fluid Science 26 (2002), pp. 677–681.
[3] V. Bermúdez, R. Payri, F.J. Salvador, and A.H. Plazas, *Study of the influence of nozzle seat type on injection rate and spray behaviour*, Proceedings of the Institution of Mechanical Engineers, part D: Journal of Automobile Engineering 219 (2005), pp. 677–689.
[4] O. Chiavola and F. Palmieri, *Modeling needle motion influence on nozzle flow in high pressure injection systems*. SAE Paper 2007 00–0250.
[5] J.M. Desantes, R. Payri, J.M. García, and F.J. Salvador, *A contribution to the understanding of isothermal diesel spray dynamics*, Fuel 86 (2007), pp. 1093–1101.
[6] G.M. Faeth, L.P. Hsiang, and P.K. Wu, *Structure and breakup properties of sprays*, International Journal of Multiphase Flow 21 (1995), pp. 99–127.
[7] F.P. Kärrholm, H. Weller, and N. Nordin, *Modelling injector flow including cavitation effects for diesel applications*. proceedings of FEDSM2007, 5th Joint ASME/JSME Fluids Engineering Conference, July 30- August 2, San Diego, California, USA.
[8] J.W. Lee, K.D. Min, K.Y. Kang, C.S. Bae, E. Giannadakis, M. Gavaises, and C. Arcoumanis, *Effect of piezo-driven and solenoid-driven needle opening of common rail diesel injectors on internal nozzle flow and spray development*, International Journal of Engine Research 7 (2006), pp. 489–502.
[9] T. Oda, M. Hiratsuka, Y. Goda, S. Kanaike, and K. Ohsawa, *Experimental and numerical investigation about internal cavitating flow and primary atomization of a large-scaled vco diesel injector with eccentric needle*. ILASS-Europe 2010, 23rd Annual Conference on Liquid Atomization and Spray Systems, Brno, Czech Republic, September 2010.
[10] S.H. Park, H.K. Suh, and C.S. Lee, *Effect of bioethanol-biodiesel blending ratio on fuel spray behavior and atomization characteristics*, Energy & Fuels 23 (2009), pp. 4092–4098.
[11] F. Payri, R. Payri, F.J. Salvador, and J. Martínez-López, *A contribution to the understanding of cavitation effects in diesel injector nozzles through a combined experimental and computational investigation*, Computers & Fluids 58 (2012), pp. 88–101.
[12] R. Payri, J.M. García, F.J. Salvador, and J. Gimeno, *Using spray momentum flux measurements to understand the influence of diesel nozzle geometry on spray characteristics*, Fuel 84 (2005), pp. 551–561.
[13] R. Payri, F.J. Salvador, J. Gimeno, and J. De la Morena, *Effects of nozzle geometry on direct injection diesel engine combustion process*, Applied Termal Engineering 29 (2009), pp. 2051–2060.
[14] R. Payri, F.J. Salvador, P. Martí-Aldaraví, and J. Martínez-López, *Using one-dimensional modeling to analyse the influence of the use of biodiesels on the dynamic behavior of solenoid-operated injectors in common rail systems: Detailed injection system model*, Energy Conversion and Management 54 (2012), pp. 90–99.

[15] F.J. Salvador, J. Gimeno, J. De la Morena, and M. Carreres, *Using one-dimensional modeling to analyse the influence of the use of biodiesels on the dynamic behavior of solenoid-operated injectors in common rail systems: Results of the simulations and discussion*, Energy Conversion and Management 54 (2012), pp. 122–132.

[16] S. Unverdi and G. Tryggvason, *A front-tracking method for viscous, incompressible, multi-fluid flows*, Journal of Computational Physics 1 (1992), pp. 25–37.